3. T. Cebeci, A. M. O. Smith, and G. Mosinskis, AIAA J., 8, No. 11, 1973-1982 (1977).
4. R. L. Simpson, Y. T. Chew, and B. G. Shivarprasad, J. Fluid Mech., 113, 23-51 (1981).
5. R. L. Simpson, J. Fluid Eng., 103, 520-533 (1981).
6. E. M. Khabakhpasheva and G. I. Efimenko, Structure of Forced and Thermogratitational Flows [in Russian], Novosibirsk (1983), pp. 5-31.
7. V. V. Zyabrikov and L. G. Loitsyanskii, Izv. Akad. Nauk SSSR, Mekh. Zhidk. Gaza, No. 5, 46-53 (1987).
8. D. Cowles, Boundary Layer Problems and Aspects of Heat Transfer [in Russian], Moscow, Leningrad (1960), pp. 138-147.
9. K. K. Fedyaevskii, A. S. Ginevskii, and A. V. Kolesnikov, Calculation of the Turbulent Boundary Layer of an Incompressible Fluid [in Russian], Leningrad (1973).
10. Proceed. Comp. of Turbulent Boundary Layer, AFOSR-I Fr., Stanford Conf. Themosciences Division, Dep. of Mech. Eng., California, USA, Vol. 2 (1969).
11. R. A. Galbraith and M. R. Head, Aeronaut. Q., 26, (pt. 2), 133-154 (1975).
12. B. L. Reeves, AIAA J., 12, No. 7, 932-939 (1974).
13. M. J. Nituch, S. Sjolander, and M. D. Head, Aeronaut. Q., 29, No. 3, 207-225 (1978).
14. G. I. Efimenko and E. M. Khabakhpasheva, Gradient and Separated Flows [in Russian], Novosibirsk (1976), pp. 49-68.
15. O. N. Kashinskii, S. S. Kutateladze, V. A. Mukhin, and V. E. Nakoryakov, Zh. Prikl. Mekh. Tekh. Fiz., No. 6, 92-96 (1974).
16. V. K. Lyakhov, M. I. Deveterikova, Yu. F. Ukrainskii, and S. Ya. Grabarnik, "Violation of the 'wall law' in flows with a positive pressure gradient," Submitted to VINITI 29.04.82, No. 2124-82 (1982).
17. H. Lidwieg and W. Tillman, Ing. Arch., 17, 288-299 (1949).
18. B. Ya. Kader and A. M. Yaglom, "Effect of roughness and a longitudinal pressure gradient on turbulent boundary layers," Itogi Nauki Tekh. Mekh. Zhidk. Gaza, 18, 3-111 (1984).

CALCULATION OF THE CHARACTERISTICS OF COUNTERCURRENT AXISYMMETRIC JETS

V. A. Dvoinishnikov, M. A. Laryushkin, and A. N. Rozhko

UDC 532.517.4

On the basis of analysis and generalization of experimental data, a method is proposed for calculating the parameters of the interaction of two coaxial jets flowing in opposite directions from circular nozzles of different diameters.

The operation of many types of equipment (boilers and dryers, high-pressure combustion chambers, etc.) is based on the interaction of countercurrent jets. In light of this, knowledge of the general laws governing their propagation acquires particular importance.

The literature data [1-3] shows that the propagation of a jet in an infinite opposing flow has been studied the most intensively, while there are almost no generalizing relations which describe the interaction of jets of finite dimensions.

We will examine the case of the coaxial interaction of two axisymmetric jets flowing in opposite directions from circular nozzles. The experiments were conducted on a unit with a fixed distance between the nozzles L_{ax} = 320 mm. The diameter of the large nozzle D was left constant and equal to 80 mm. The diameter of the small nozzle d was varied from 10 to 30 mm. Air was delivered to the system by a separate blower. The ratio of the impulses of the air jets $\bar{q} = \rho u^2/\rho_{\ell d} u_{\ell d}^2$ in the experiment was 0.2-4, which corresponded to a change in the Reynolds number $Re_{\ell d} = (4\text{-}2.5)\cdot 10^5$ for the large jet and $Re = (2\text{-}10)\cdot 10^4$ for the small jet.

Moscow Energy Institute. Translated from Inzhenerno-Fizicheskii Zhurnal, Vol. 56, No. 5, pp. 725-729, May, 1989. Original article submitted November 16, 1987.

 0022-0841/89/5605-0508$12.50

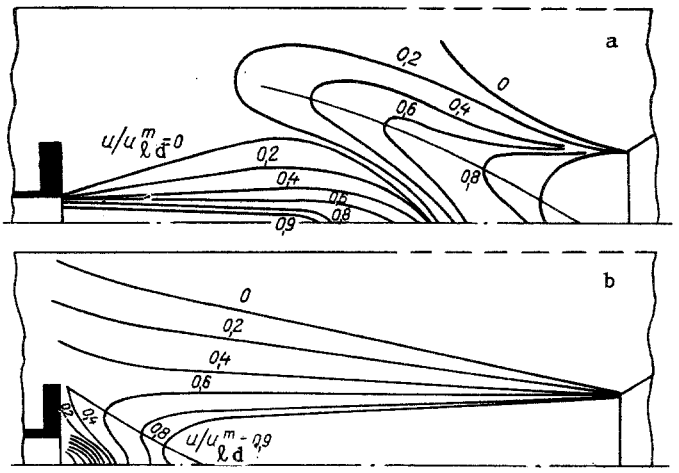

Fig. 1. Field of isotachs in a longitudinal section at $\bar{q} > \bar{q}_0$ (a) and $\bar{q} < \bar{q}_0$ (b).

In the experiment we conducted, we continuously recorded the flow parameters by means of a semi-automatic system [4]. A pneumatic signal received from a T-shaped pilot static head was converted to an electrical signal by an induction pressure transducer and recorded by a two-coordinate potentiometer. The potentiometer also received a signal from a linear slide resistance installed on a traversing gear, this signal indicating the position of the primary transducer.

The test results showed that the profile of longitudinal velocity changes in both the longitudinal and transverse directions in the region of the jet interaction. Its change is symmetrical relative to the long axis, while it is divided into two regions in the transverse direction: propagation of the small-diameter jet and propagation of the large-diameter jet. With increasing distance from the edge of the small-diameter nozzle, deformation proceeds in the direction of contraction of the profile and a reduction in its width. The point of intersection of the profile with the x-axis corresponds to zero velocity and is taken as the boundary between the jets.

In regard to the character of change in velocity, the interaction of jets of finite dimensions is nearly the same as the development of a jet in an infinite opposing flow [5]. However, the qualitative characteristics are different. This applies particularly to the change in the axial velocity of the small-diameter jet. Velocity is unchanged for a certain distance from the small-diameter nozzle, but it then decreases. The curve of the change in axial velocity is concave, in contrast to the convex form seen in the development of a jet in an infinite opposing flow [6]. The change in axial velocity indicates the existence of initial and main sections here. Analysis of the velocity profile on the main section of the small-diameter jet in the dimensionless coordinates $u/u_m = f(y/y_{0.5})$ shows that it can be described by a single relation. The latter is evidence of the affinity of the velocity fields, regardless of the flow regime or the ratio of the initial diameters of the jets.

Study of the fields of isotachs constructed from the velocity profiles in different cross sections showed that there are two cases of development of the small-diameter jet in the investigated range of $\bar{q}$ (Fig. 1).

In the first case (Fig. 1a), this jet develops in a manner similar to the jet in an infinite opposing flow; there is initially an increase in the transverse dimensions of the jet, and its boundaries become nearly linear. The width of the jet then decreases, and the jet becomes stretched out along the axis. The mechanism of jet development here is as follows: first it ejects the medium from the surrounding space; then, as a result of stagnation, the jet material separates and is entrained by the opposing flow.

In the second case (Fig. 1b), the small-diameter jet is "run over," as it were. It is pressed by the opposing flow against the edge of the nozzle. Its maximum width occurs in its initial section, and the width of the jet decreases as it develops. Here, stagnation of the jet begins directly at the nozzle edge.

The existence of each of the above-described cases is identified with a certain limiting value of relative impulse $\bar{q}_0$. At $\bar{q} > \bar{q}_0$, the first case of jet development prevails. At $\bar{q} < \bar{q}_0$, the second case exists.

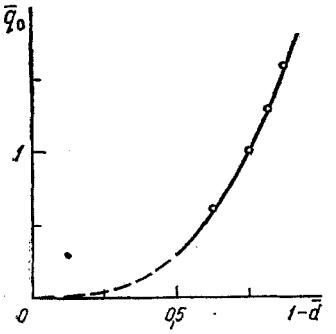

Fig. 2

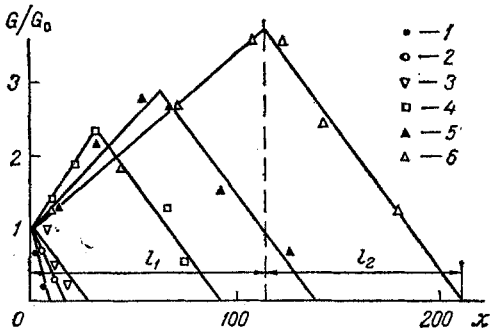

Fig. 3

Fig. 2. Dependence of $\bar{q}_0$ on the relative diameter of the jets.

Fig. 3. Change in the mass of the smaller jet along the axis, d = 30 mm: 1) q = 0.22; 2) 0.4; 3) 0.6; 4) 0.96; 5) 1.15; 6) 1.4. x, mm.

TABLE 1. Relations for Calculation of the Main Parameters of the Jets

Parameter	First zone	Second zone
	Small-diameter jet	
$\bar{l}_i = l_i/d$	$\bar{l}_1 = 40\bar{d}^2 (\bar{q}_*)^{5/3}$, where $\bar{q}_* = \bar{q} - \bar{q}_0$	$\bar{l}_2 = 5{,}1\bar{d}\,(\bar{q})^{4/3}$
$2\bar{r}_i = 2r_i/d$	$2\bar{r}_1 = 1 + 25{,}6\bar{x}\bar{d}^2\bar{q}_*$, where $\bar{x} = x/l_1$	$2\bar{r}^2 = (1 + 25{,}6\bar{d}^2\,\bar{q}_*)[1-\varphi(x)]^{0,8}$, where $\varphi(x) = (x - l_1)/l_2$
$\bar{G}_i = G_i/G_0$	$G_1 = 2\bar{r}_1$, where $2\bar{r}_1$, see part 2	$\bar{G}_2 = G_1(l_1)\,[1 - \varphi(x)]$, where $\varphi(x)$, see part 2
$\bar{u}_i = u_i/u(l_i)$	$\bar{u}_1(x) = 1$	$\bar{u}_2 = [1 - \psi(x)]^{0,7}$, where $\psi(x) = \left(\frac{x - l_1}{l_2}\right)^{3/2}$
	Large-diameter jet	
$\bar{L}_i = L_i/D$	$\bar{L}_1 = L_{ax}[1 - 3{,}6\bar{d}^2 (q_*)^{3/2}]/4$, where $L_{ax} = 320$ mm is the distance between nozzles	$\bar{L}_2 = \bar{L}_{ax} - \bar{L}_1 - l_1\bar{d}$,
$2\bar{B}_i = 2B_i/D$	$2\bar{B}_1 = 0$	$2\bar{B}_2 = [2\bar{r}_2 + 2(1 - \bar{d})] \times [1 - \varepsilon(x)]^{1,1}$, where $\varepsilon(x) = \left(\frac{L_{ax} - x - L_1}{L_2}\right)^{1,35}$
$\bar{U}_{axi} = U_{axi}/U_m$	$\bar{U}_{ax_1} = 1$	$\bar{U}_{ax_2}\,[1 - \varepsilon^{1,5}(x)]^{0,6}$
$\bar{U}_{mi} = \frac{U - U(L_2)}{U_m - U(L_2)}$	$\bar{U}_{m1} = 1$	$\bar{U}_{m2} = [1 - \varepsilon(x)]^{2/3}$
	$U(L_2) = 0{,}75 - 0{,}85\bar{d}\,\bar{q}$.	

One feature of the interaction of jets of finite dimensions is that the large-diameter jet also undergoes deformation. Its width initially increases. This is followed by a sudden expansion of the jet. Its boundaries become curvilinear and are similar to the boundaries seen in flow about solids.

Study of the structure of the interacting jets showed that each of them has two characteristic zones of development in the case $\bar{q} > \bar{q}_0$. The first is referred to as the zone of free development, while the second is the deformation zone.

The free-development zones for the large- and small-diameter jets correspond to their initial section. For the small-diameter jet, the length of this zone coincides with the ejection section. As noted above, its boundaries are nearly linear in this case, while the angle of divergence depends on the discharge conditions. The boundaries of the large-diameter jet are also linear in the first zone, and their inclination to the axis is close to the inclination characteristic of the submerged jet. Analysis of the velocity profile on this section of motion of the large-diameter jet in dimensionless coordinates showed that it is identical to the profile of the submerged jet.

The deformation zone of the small-diameter jet is located between its initial section and the section where it loses its individuality. This section is determined from the point of intersection of the zero isotach with the axis of the jet.

For the large-diameter jet, the second zone is located between the sections corresponding to the initial regions of the interacting jets. When the small-diameter jet is discharged with the relative impulse $\bar{q} < \bar{q}_0$ (second case), the initial section of the jet is nearly absent, and it has only one zone — the deformation zone.

Analysis of the experimental data showed the change in the quantitative characteristics of the jet. The following were used as the main parameters to describe the kinematic structure of the jet: the relative impulse $\bar{q}$, velocity u, discharge G, width 2r, the length of the flow zone ℓ_1, ℓ_2, and the range of the jet ℓ. Some of these parameters are of a specific nature and require some explanation. Thus, the range of the jet ℓ is equal to the sum of the lengths of the first ℓ_1 and the second ℓ_2 flow zones in accordance with the proposed schematization at $\bar{q} > \bar{q}_0$. At $\bar{q} < \bar{q}_0$, $\ell = \ell_2$. As the width of the jet 2r, we took the distance between the boundaries of the jet in the corresponding cross section. As the main parameter of interaction, we used the relative impulse $\bar{q}_0$.

In tests we conducted, we determined the relative impulse $\bar{q}_0$. This quantity defines the existence of each of the two cases of development of the small-diameter jet. The value of $\bar{q}_0$ depends on the ratio of the initial diameters of the jets $\bar{d} = d/D$ and increases with a decrease in the latter (Fig. 2). The length of the first flow zone is zero in the case $\bar{q} < \bar{q}_0$, so that the range of the jet ℓ is equal to ℓ_2. At $\bar{q} > \bar{q}_0$, the range is the sum of the lengths of the first and second flow zones. The tests showed that the length of the zones depends on the ratio of both the impulses and the initial diameters $\bar{d}$ of the interacting jets. Other conditions being equal, an increase in $\bar{d}$ is accompanied by an increase in the range of the jet.

The discharge characteristics of the jets are of particular interest. Figure 3 shows the change in the mass of the small-diameter jet. The ratio of the running discharge G to the initial discharge G_0 along the jet x at first increases linearly (ejection section) and then decreases (deformation section). At the transition point, jet discharge is maximal. This point is located in the jet section in which the transition occurs from the first to the second flow zone, in accordance with the proposed schematization, and it can be used to more accurately determine this boundary (ℓ_1). It can be seen from Fig. 3 that an increase in $\bar{d}$ leads to an increase in the intensity of ejection in the first zone. In the second flow zone (ℓ_2), the character of change in G/G_0 is independent of $\bar{d}$ and $\bar{q}$.

The completed studies have made it possible to propose a theoretical scheme which considers features of the interaction of oppositely-directed jets. Table 1 shows empirical relations obtained from approximation of test data for calculation of the main characteristics of countercurrent axisymmetric jets.

The theoretical relations for the two characteristic flow zones of the small- and large-diameter jets are valid under the following conditions: $0.125 \leq \bar{d} \leq 0.375$; $L_{ax}/D \leq 4.0$; $0.58 \leq \bar{q}_0 \leq 1.6$; $\bar{q}_m \leq 0.43(\bar{d})^{-4/3}$.

NOTATION

d, D, diameter of the nozzles for the small- and large-diameter jets; ρ, density; x, y, coordinates; u, U, averaged longitudinal component of velocity of the small- and large-diameter jets; L_{ax}, distance between nozzles; $\bar{q}$, relative impulse; G, mass rate of the medium; 2r, width of the jet; ℓ_i, L_i, lengths of the flow zones of the small- and large-diameter jets, where i = 1, 2; ℓ, range of the jet; 2B, distance between corresponding points of lines of maximum velocity of the large-diameter jet. Indices: 0, initial state; m, maximum value; ax, value on the axis; ℓd, large-diameter jet; $y_{0.5}$, distance from the axis to the point at which the velocity is equal to half the velocity on the axis.

LITERATURE CITED

1. Kh. N. Sui, Izv. Akad. Nauk Est. SSR, Tekh. Fiz. Mat. Nauk, 11, No. 4, 215-222 (1962).
2. A. N. Sekundov, Investigation of Turbulent Jets of Air, Plasma, and Real Gas [in Russian], (1967), pp. 131-142.
3. Kh. N. Sui and Yu. V. Ivanov, Izv. Akad. Nauk Est. SSR Tekh. Fiz. Mat. Nauk, 8, No. 2, 88-96 (1959).
4. M. A. Laryushkin and V. P. Knyaz'kov, Izv. Vyssh. Uchebn. Zaved. Énerg., No. 12, 83-86 (1983).
5. L. A. Vulis and T. P. Leont'ev, Izv. Akad. Nauk Kaz. SSSR, Ser. Énerg., 9, 109-122 (1955).
6. A. S. Ginevskii, Prom. Aérodin., 23, 96-104 (1962).

GRADIENT NUMERICAL-ANALYTICAL METHOD FOR SOLUTION OF THE NAVIER–STOKES EQUATIONS FOR A VISCOUS INCOMPRESSIBLE FLUID

A. A. Shmukin and R. A. Posudievskii

UDC 532.5

A method is presented for solution of the Navier–Stokes equations in an extremal formulation based on a joint application of Pontryagin's maximum principle and a representation of the unknown functions in the form of power series.

The system of Navier–Stokes equations describing plane laminar motion of a viscous incompressible fluid in velocity–pressure variables has the form

$$\frac{du}{\partial t}+u\frac{\partial u}{dx}+v\frac{\partial u}{\partial y}=-\frac{\partial P}{\partial x}+\frac{1}{\mathrm{Re}}\left(\frac{\partial^2 u}{\partial x^2}+\frac{\partial^2 u}{\partial y^2}\right), \tag{1}$$

$$\frac{\partial v}{\partial t}+u\frac{\partial v}{\partial x}+v\frac{\partial v}{\partial y}=-\frac{\partial P}{\partial y}+\frac{1}{\mathrm{Re}}\left(\frac{\partial^2 v}{\partial x^2}+\frac{\partial^2 v}{\partial y^2}\right), \tag{2}$$

$$\frac{\partial u}{\partial x}+\frac{\partial v}{\partial y}=0. \tag{3}$$

In solving the system (1)-(3), as a rule, one replaces the continuity equation by the Poisson equation for the pressure. It was noted in [1] that the main difficulty in this case consists in integrating the Poisson equation with Neumann type boundary conditions (as the boundary condition one uses an expression for projection of momentum on a wall). A part of the algorithms for solving the Navier–Stokes equations is connected with their integration in stream function-vorticity variables. Moreover, specific difficulties arise in calculation of the boundary conditions for the vorticity, which are not given from the physical conditions. We present below an iterational algorithm for solving Eqs. (1)-(3) which makes use of the natural boundary conditions and does not require integration of the Poisson equation.

We introduce the functional

$$J_0=\int_0^{t_\kappa}\left[\oint_\Gamma u_n ds\right]^2 dt. \tag{4}$$

By decomposing the region with the moving fluid into elementary regions bounded by lines joining nodes of a grid, we can replace the problem of finding the pressure from the condition for a minimum of functional (4) for each elementary region by the solution of Eqs. (1), (2). As a result, along with the pressure we shall determine the velocity components.

Institute of Engineering Mechanics, Academy of Sciences of the Ukrainian SSR, Dnepropetrovsk.
Translated from Inzhenerno-Fizicheskii Zhurnal, Vol. 56, No. 5, pp. 730-735, May, 1989. Original article submitted November 11, 1987.

 0022-0841/89/5605-0512$12.50